Diagnosis of Oscillations in an Industrial Mineral Process Using Transfer Entropy and Nonlinearity Index ⋆

Brian Lindner * **Moncef Chioua** ** **J.W.D Groenewald** ***
Lidia Auret * **Margret Bauer** ****

* *Department of Process Engineering, Stellenbosch University, Private Bag X1, Matieland 7602, South Africa (e-mail: blindner@sun.ac.za)*
** *ABB Corporate Research, Ladenburg, Germany*
*** *Anglo American plc., Johannesburg, South Africa*
**** *Department of Electrical, Electronic and Computer Engineering, University of Pretoria, Pretoria 0002, South Africa*

Abstract: Oscillations in mineral processes can propagate through multiple units, causing important controlled variables to deviate from their set points and degrade control performance. Root cause diagnosis of oscillations enables corrective action to return to desired operation.
Numerous data-based methods for diagnosis of oscillations have been developed. Transfer entropy and the nonlinearity index are popular techniques that have been proven effective for oscillation diagnosis for a number of processes. Transfer entropy is a causality analysis technique. Causal relationships between measured variables are inferred, which allows the oscillation propagation path to be traced. The nonlinearity index ranks variables according to their nonlinearity content. The assumption is that the nonlinearity is greatest close to the oscillation source, since the process acts as a linear filter as the oscillation propagates.
An oscillation propagating through multiple control loops in a mineral processing plant was identified. The validity of transfer entropy and nonlinearity index for oscillation diagnosis was compared, highlighting their benefits and pitfalls when applied to a real industrial case study. The results revealed contradictory root causes for transfer entropy and the nonlinearity index. Consideration of process knowledge indicated that the transfer entropy results were consistent with the material flow and control structure. This indicates that transfer entropy accurately traced the oscillation propagation, while the nonlinearity index gave erroneous results. Nonlinear behaviour occurring in the process caused nonlinear trends to develop downstream of the root cause, making the assumptions of the nonlinearity index invalid. This result demonstrates the need for careful analysis of fault diagnosis results using expert knowledge of the process.

Keywords: Oscillation, fault diagnosis, causality analysis, mineral processing, nonlinearity.

1. INTRODUCTION

Mineral processes employ advanced control strategies to operate multiple units at desired conditions for optimisation of production rate and grade. Hundreds of control loops are typically used in such a control strategy. Satisfactory operation of these loops is essential to ensure optimal process conditions are maintained. Oscillations in these processes can cause fluctuations in the controlled variables of multiple units as the oscillation propagates through the process. Swift diagnosis and corrective action of such oscillations is essential to ensure efficient mineral beneficiation.

Once an oscillation has propagated through the process and manifested in multiple measured variables, it is difficult to distinguish the root cause of the oscillation from downstream variables that show symptoms of the oscillation. Numerous data-based methods for diagnosis of plant wide oscillations have been developed. Causality analysis techniques have been employed for oscillation diagnosis, including transfer entropy (Bauer et al., 2007), Granger causality (Yuan and Qin, 2014), and cross-correlation (Bauer and Thornhill, 2008). These techniques determine causal relationships between measured variables, which allows the propagation path of the oscillation to be traced. The nonlinearity index approach (Thornhill, 2005) ranks variables according to their nonlinearity content. The assumption is that the nonlinearity is greatest close to the source of the oscillation. This assumption is justified when the process acts as a linear filter as the oscillation propagates.

Some techniques may perform better than others depending on the scenario being diagnosed. For a process engineer, selecting the appropriate technique from the various tools available may be difficult. Understanding the benefits limitations of techniques can help with this decision. Better decision making in the application of fault diagnosis tool will lead to more successful and reliable diagnosis of

⋆ The authors gratefully acknowledge the support of Anglo American Platinum.

oscillations in industrial processes. In this paper transfer entropy and the nonlinearity index are used to diagnose an oscillation propagating through multiple control loops in a mineral process plant. The nonlinearity index was chosen because it is a well established oscillation diagnosis technique. Transfer entropy was chosen because it is a popular technique in the developing field of causality analysis Yang and Xiao (2012). Their validity for oscillation diagnosis is compared, highlighting the benefits and pitfalls when applied to a real industrial case study. Data-based techniques for oscillation diagnosis can swiftly provide indications of the root cause. However, the need for careful consideration of process knowledge for interpretation and verification of the results is apparent.

This paper is structured as follows: Section 2 presents techniques for oscillation diagnosis; Section 3 describes the case study of the oscillation in a flotation circuit; Section 4 presents the results of application of transfer entropy and nonlinearity index for oscillation diagnosis; and finally Section 5 presents the conclusions and some some further recommendations.

2. METHODS

Numerous data-based methods for diagnosis of plant wide oscillations have been developed. Transfer entropy and the nonlinearity index are popular data-based oscillation diagnosis techniques that have been proven effective for various processes. These two methods are tested in this paper and described in this section.

2.1 Transfer entropy

Causality analysis techniques determine causal relationships between measured variables in a process. This allows tracing of the propagation path of an oscillation through a process. Transfer entropy is an information-theoretic interpretation of causality between two variables. This technique has been proven effective for oscillation diagnosis in chemical processes (Bauer et al., 2007; Duan, 2014; Landman and J\"ams\"a-Jounela, 2016). Transfer entropy represents the reduction in uncertainty of variable $\mathbf{Y}$ when including past values of variable $\mathbf{X}$. The transfer entropy from $\mathbf{X}$ to $\mathbf{Y}$ can be calculated as shown in Equation 1.

$$T_{x|y} = \sum p(y_{i+h}, \mathbf{Y}_i^{(K)}, \mathbf{X}_i^{(L)}) \cdot \log \frac{p(y_{i+h}|\mathbf{Y}_i^{(K)}, \mathbf{X}_i^{(L)})}{p(y_{i+h}|\mathbf{Y}_i^{(K)})} \quad (1)$$

In Equation 1: $p(a, b)$ represents the joint probability distribution function (PDF) between a and b; $p(a|b)$ represents the conditional PDF of a given b; h is the prediction horizon; $\mathbf{X}_i^{(K)} = [\mathbf{x}_i, \mathbf{x}_{i-\tau}, ..., \mathbf{x}_{i-(K-1)\tau}]$ and $\mathbf{Y}_i^{(L)} = [\mathbf{y}_i, \mathbf{y}_{i-\tau}, ..., \mathbf{y}_{i-(L-1)\tau}]$ are the embedded vectors of $\mathbf{X}$ and $\mathbf{Y}$ with embedding dimensions, K and L respectively, and sampling period, τ. The numerator of the logarithmic term in Equation 1 represents the probability that $\mathbf{Y}$ has a certain value when past values of both $\mathbf{Y}$ and $\mathbf{X}$ are known. The denominator of the logarithmic term in Equation 1 represents the probability that $\mathbf{Y}$ has a certain value when past values of only $\mathbf{Y}$ are known. When $\mathbf{Y}$ is independent of $\mathbf{X}$, the numerator and denominator are equal, and the logarithm reduces to $\log(1) = 0$, giving $T_{y\to x} = 0$. When prediction of $\mathbf{Y}$ is improved by inclusion of $\mathbf{X}$, the numerator is greater than the denominator and $T_{x\to y} > 0$. The PDFs can be calculated using kernel density estimation. A causality measure comparing the influence of x on y with the influence of y on x can be calculated according to Equation 2 (Bauer et al., 2007).

$$T_{x\to y} = T_{y|x} - T_{x|y} \quad (2)$$

Stochasticity of the time series means that non-zero values will be obtained even when there is no causal relationship. Hypothesis tests to determine the statistical significance of the values obtained need to be employed. A significance threshold for the transfer entropy can be calculated using the method suggested by Kantz and Schreiber (1997), where Monte Carlo simulations are used to generate numerous surrogate time series for each variable. The transfer entropy between the surrogates is then calculated, and a 6-sigma threshold is set, as shown in Equation 3.

$$S_{x\to y} = \mu_{T^{surr}_{x\to y}} + 6 * \sigma_{T^{surr}_{x\to y}} \quad (3)$$

Application of transfer entropy for oscillation diagnosis is achieved by the following steps:

Step 1) Calculate $T_{x\to y}$, using Equations 1 and 2, for every pair of variables. A connectivity matrix, $\mathbf{C}$, can be constructed, where $C_{i,j}$ is the transfer entropy between variables i and j, $T_{i\to j}$.

Step 2) Create M surrogate time series for each variable. Calculate transfer entropy between the surrogates of pairs of variables. The significance threshold for each pair is then calculated with Equation 3. Entries in the connectivity matrix where $T_{i\to j} < S_{i\to j}$ are set to 0.

Step 3) Construct a connectivity map from $\mathbf{C}$, where nodes represent the variables, and edges represent connections between them. This map illustrates the propagation path of the oscillation. The first variable in this propagation path is closest to the root cause of the oscillation.

2.2 Nonlinearity index

Thornhill (2005) developed a nonlinearity index that ranks variables according to the nonlinearity of their time series. A plant acts as a mechanical low pass filter (Thornhill, 2005) as the oscillation propagates to different variables. The low-pass process dynamics remove the higher harmonics in the trends and destroy the phase-coupling. This makes the waveforms more sinusoidal and more linear the further away from the root cause the variable is. Therefore the variables with the highest nonlinearity index are assumed to be closest to the root cause.

The basis of the nonlinearity test is comparison of the predictability of the time series trend to that of generated surrogate trends (Thornhill, 2005). The nonlinearity index can be calculated using the following steps:

Step 1) Embedded matrix as shown in Equation 4.

$$\mathbf{X} = \begin{pmatrix} x(1) & x(2) & \cdots & x(E) \\ x(2) & x(3) & \cdots & x(E+1) \\ x(3) & x(4) & \cdots & x(E+2) \\ \cdots & \cdots & \cdots & \cdots \\ x(l-E+1) & x(l-E+2) & \cdots & x(l) \end{pmatrix} \quad (4)$$

Step 2) For each row of $\mathbf{X}$ find the indices j_p of k nearest neighbour rows having the k smallest values of $||\mathbf{x}_{j_p} - \mathbf{x}_i||$.

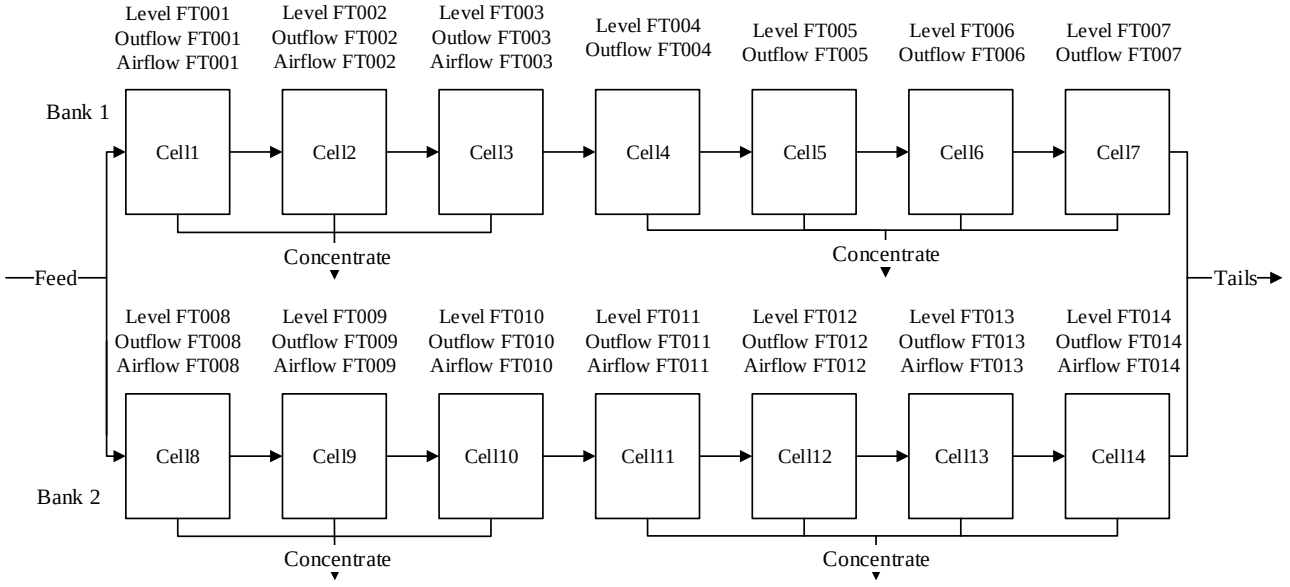

Fig. 1. Simplified process flow diagram of flotation circuit under consideration. Two banks of seven flotation cells in series make up the circuit. Each cell's outflow flows into the subsequent cell.

Step 3) The sum of squared errors is then calculated as shown in Equation 5.

$$\Gamma_{test} = \sum_{i=1}^{l-H}(x(i+H) - \frac{1}{k}\sum_{p=1}^{k} x(j_p+H))^2 \qquad (5)$$

Step 4) M surrogate data sets are generated, and then steps 1 through 3 are repeated to create surrogate predictions errors Γ_{surr}. Surrogates are generated by taking the discrete Fourier transform (DFT) of the data, randomising the arguments and applying the inverse DFT.

Step 5) The nonlinearity is diagnosed using a three sigma test statistic as shown in Equation 6 (Thornhill, 2005), where $\sigma_{\Gamma_{surr}}$ is the standard deviation of the reference distribution, and the abr indicates the mean value.

$$N = \frac{\bar{\Gamma}_{surr} - \Gamma_{test}}{3\sigma_{\Gamma_{surr}}} \qquad (6)$$

When $N > 1$, nonlinearity is inferred, while $N < 1$ indicates linearity. Larger values of N indicate stronger nonlinearity.

Step 6) Rank variables according to their nonlinearity index. The variables with the largest nonlinearity index are considered closest to the source of the oscillation.

3. CASE STUDY

Oscillations in a flotation circuit in a mineral concentrator plant were observed. To provide sufficient context for diagnosis of the oscillations, the operation and control of the circuit is described, and the trends of the variables showing oscillations are presented. To encourage the development and testing of different control performance monitoring methods on real industrial data, the data for this case study has been made available on the industrial data repository on the website for the South African Council for Automation and Control. The case study can be found at: 'sacac.org.za/resources/' under 'PID Data/Plantwide data/plantwide_oscillation.csv'.

3.1 Flotation circuit operation and control

Flotation is used to separate valuable mineral particles from gangue particles in a concentrator process. Separation is achieved by selectively imposing hydrophobicity on the valuable mineral particles, so that they will attach to air bubbles and float to the top of the cell (Wills and Finch, 2016). A flotation circuit is a series of flotation cells. A simplified process flow diagram of the flotation circuit under consideration is shown in Figure 1. This flotation circuit consists two parallel banks, each with seven flotation cells in series. The concentrate from the first three cells of each bank are combined, and the concentrate from the last four cells are combined. The outflow (tails) from each cell flows into the following cell. Finally the combined tails are combined and processed further in downstream units.

A flotation circuit control strategy to stabilise the mass pull and optimise the final concentrate grade of the circuit is implemented in a layered approach (Muller et al., 2010). The first layer utilises PID feedback loops for regulatory control of the cell levels and air addition rate. The cell outflows are used to control cell levels using a multivariable level controller that considers interaction of upstream cells on downstream cells to compensate for disturbances that could propagate down a series of cells. This multivariable level controller allows all control valves in the circuit to act simultaneously. The second layer is a supervisory control layer to stabilise the individual cell and overall circuit mass pulls by manipulating reagent addition, froth depth (by manipulating cell level set points) and air addition rate. This control layer implements a fuzzy logic rules-based expert controller. The third layer is an optimisation layer

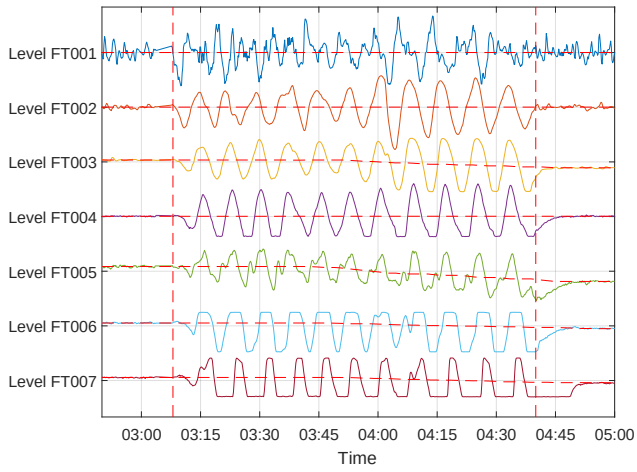

(a) Bank 1 levels. Red lines indicates set-points.

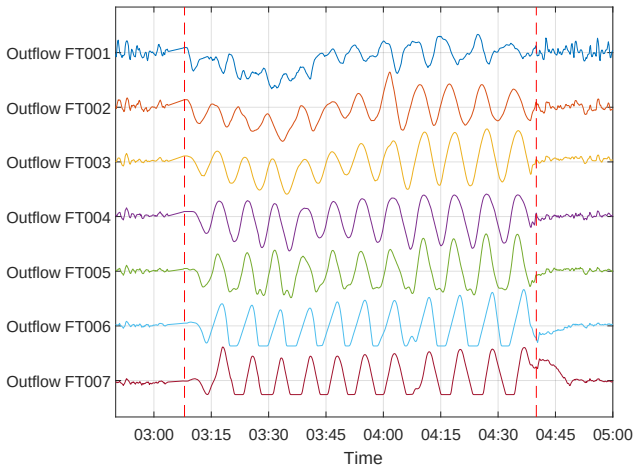

(b) Bank 1 outflows.

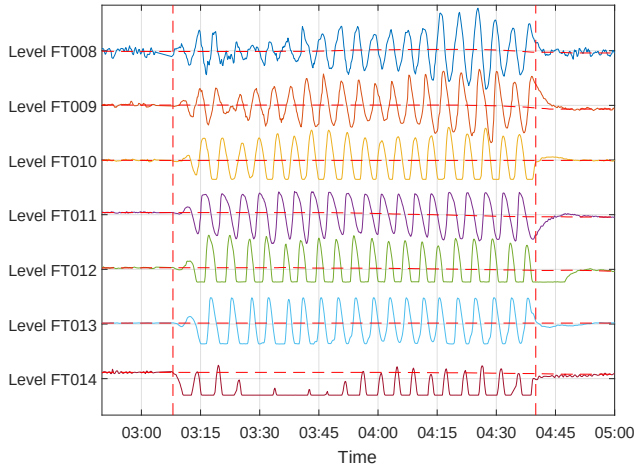

(c) Bank 2 levels. Red lines indicates set-points.

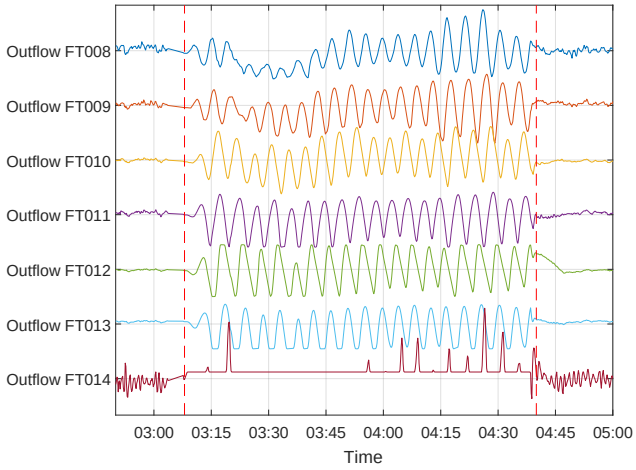

(d) Bank 2 outflows.

Fig. 2. Circuit variables showing oscillatory behaviour. Vertical dashed lines indicate onset and end of oscillations.

that optimises the final concentrate grade by manipulating the set-points of the mass pulls. A model predictive control strategy is implemented to achieve this.

3.2 Oscillatory variables

Figure 2 plots the levels and outflows in the flotation circuit. The oscillations propagated through the circuit, affecting both the controlled variables (CVs), the levels, and manipulated variables (MVs), the outflows. Processing units directly upstream and downstream of this flotation circuit did not show any effect of the oscillation, so this oscillation was localised to this flotation circuit. The oscillation was detected from manual inspection of the plant data. Automated oscillation detection techniques are available (see Thornhill and Horch (2007) for examples). However, the oscillations in this case study were clearly observable and localised, and the focus of this article was on root cause diagnosis. Therefore oscillation detection techniques were not employed or discussed in this work.

The root cause analysis was limited to variables that displayed oscillations. These 28 variables are shown in Figure 2. The oscillation is transient, persisting for roughly 1h 30 min. The sampling time is 10s, and the number of samples is 560. Before and after the oscillation the CVs are stable and well controlled at their set-points. Variables from the processing unit directly upstream of this flotation circuit did not show effects of the oscillations.

Using the fast-Fourier transform (FFT) to find the peak oscillation frequencies (Shumway and Stoffer, 2014) it was observed that the oscillations in Bank 1 (Cells 1 to 7) were at a lower frequency than Bank 2 (Cells 8 to 14). The CVs and MVs in Bank 1 all displayed a common oscillation frequency of 0.00215 Hz (a period of 465 s). The CVs and MVs in Bank 2 all displayed a common oscillation frequency of 0.00378 Hz (a period of 266 s).

4. RESULTS AND DISCUSSION

Transfer entropy and the nonlinearity index were both applied to the dataset for oscillation diagnosis in order to compare the advantages and pitfalls of each method for industrial oscillation diagnosis. The variables displaying the oscillation were grouped according to their common

oscillation frequencies, as described in Section 3.2, so Bank 1 and Bank 2's variables were analysed separately.

4.1 Transfer entropy results

Transfer entropy was applied to the data from the flotation circuit. Default calculation parameters suggested by Bauer et al. (2007) were used. The CVs and MVs were separated, and the transfer entropy analysis was performed separately for each group, since the oscillation could propagate through both the CVs and MVs due to the control and material flow in the circuit. The results for each group were then compared to determine whether the propagation paths were consistent with each other.

The propagation paths obtained from transfer entropy applied to Bank 1's levels and outflows are shown in Figures 3a and 3b respectively. Both show a propagation path from Cell 2 to Cell 7. Neither show a causal flow from Cell 1 to Cell 2. Observing the trends for Level FT001 and Level FT002 in Figure 2, the oscillation in Level FT001 appears less pronounced than in other trends. This indicates that process noise may have obscured the causal connections. Figure 3b shows a connection from Cell 5 to Cell 4, which is contradicts the physical flow of the process. From the inspection of the trends for Cells 4 and 5 in Figure 2 it can be seen that Cell 4 showed no significant nonlinear behaviour, while Cell 5 did. For this reason the connection from Cell 4 to Cell 5 may have been obscured.

The propagation paths obtained from transfer entropy applied to Bank 2's levels and outflows are shown in Figures 3c and 3d. Fig 3c shows a propagation path from Cell 10 to Cell 13. Fig 3d shows a propagation path from Cell 8 to Cell 13. Notably, no connection is observed from Level FT008 to Level FT009 or Level FT009 to Level FT010. Figure 2c shows that the trend of Level FT008 displays a less pronounced oscillation and a bit of noise, which may have obscured the causal connection. Cell 14's level and outflow show no causal connection with other variables. Figures 2c and 2d show severe saturation for Cell 14's level and outflow. This means that the causal connection between these variables an the other variables may have been obscured.

Transfer entropy applied to Bank 1 and Bank 2's variables both indicate the oscillations originating in the first cells and propagating down the banks to the last cells. These results are compared with those of the nonlinearity index and their accuracy when considering additional process knowledge context is discussed in Section 4.3.

4.2 Nonlinearity index results

The nonlinearity index approach was applied to rank the variables according to the degree of nonlinearity. The results of the nonlinearity index are presented in Table 1. The results for Bank 1 indicate strong nonlinearity in a number of the trends. Level FT005 displayed strong nonlinearity. In Figures 2a and 2b the severe nonlinear trends for Cell 5 can be seen. The oscillations appear jagged, with a smaller peak present in each repeating peak. In contrast, Cells 1 and 2 show oscillations with a smoother sine wave form. These observation confirm the nonlinearity rankings obtained using the nonlinearity index.

For Bank 2, Cell 13 showed the highest nonlinearity index value, indicating that this cell's level was closest to the oscillation root cause. Cells 8 and 9 showed linear results, indicating they were furthest from the oscillation root cause. The trends in Figures 2c and 2d show smoother sine oscillations for Cells 8 and 9, with more jagged trends for Cells 11 and 13. Bank 1 and Bank 2 showed similar results, where the first cells showed linear oscillatory trends, and the later cells showed nonlinear behaviour. Cells 5 and 13 may be considered closest to the root cause of the oscillation according to this technique, since they displayed the largest nonlinearity indices.

Table 1. Nonlinearity index results for Bank 1 and Bank 2.

Variable	Nonlinearity Index
Bank 1	
Level FT005	2.48
Level FT007	1.97
Outflow FT005	1.92
Outflow FT007	1.88
Level FT004	1.7
Level FT006	1.57
Level FT003	1.35
Outflow FT006	1.33
Outflow FT003	1.19
Outflow FT004	1.09
Outflow FT001	Linear
Outflow FT002	Linear
Level FT002	Linear
Level FT001	Linear
Bank 2	
Level FT013	2.88
Level FT011	2.86
Level FT012	2.71
Level FT014	2.49
Level FT010	2.36
Outflow FT011	2.01
Outflow FT013	1.87
Outflow FT012	1.38
Outflow FT010	1.22
Level FT009	Linear
Outflow FT008	Linear
Level FT008	Linear
Outflow FT009	Linear

4.3 Discrepancy of different methods and further analysis

The transfer entropy results indicated that the oscillation propagated from the first cells through the circuit to the last cells, for both banks. The nonlinearity index gave contradictory results, indicating that Level FT005 and Level FT013 were closest to the sources of the oscillation for each Bank. To determine which of the methods gave the correct root cause some additional context is necessary.

An oscillation takes time to propagate through the process, due to the residence time of the cells and the transport delay between cells. The sequence of the oscillation propagation may give further insight into the propagation path. The trends for the levels were inspected to determine when the first peak of the oscillations appeared. The locations of these peaks establishes the sequence in which the oscillations appear in the cells. The start times are shown in Table 2. The start times are in mostly sequential order from

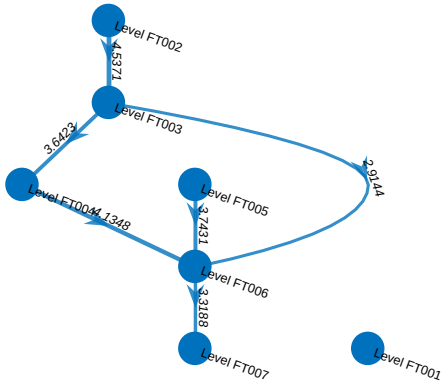

(a) Propagation path for Bank 1 levels

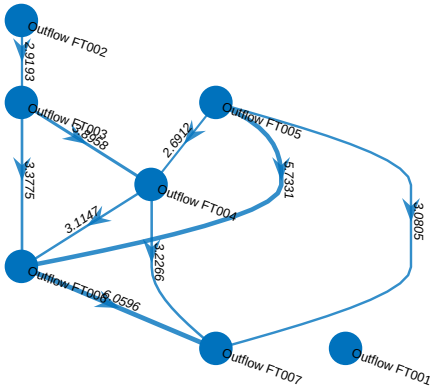

(b) Propagation path for Bank 1 outflows

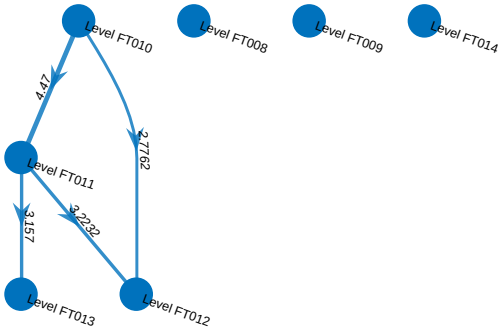

(c) Propagation path for Bank 2 levels

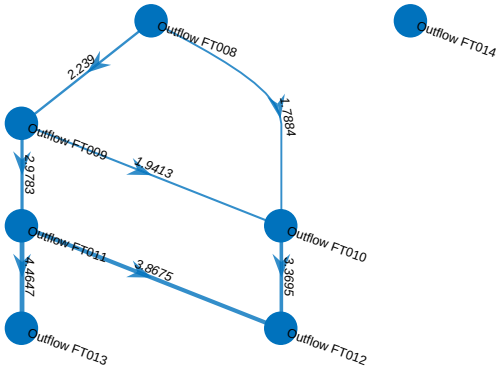

(d) Propagation path for Bank 2 outflows

Fig. 3. Propagation paths for oscillations in the flotation circuit.

the first cell to the last cell for each bank. One exception is that the start time for Level FT014 is earlier than for Level FT010, FT011, FT012, and FT013. However, in Figure 2c it can be seen that the signal for Level FT014 displays saturation, making it difficult to accurately determine the start of the oscillation. Level FT007 appears to precede Level FT006, and Level FT011 appears to precede Level FT010. However, since the difference is only one sample (with the sampling time at 10 seconds), it is difficult to determine which was first.

The sequential order of the oscillations confirms the propagation path obtained from the transfer entropy results. This indicates that the nonlinearity index failed to correctly identify the root cause. The nonlinearity index approach assumes that a nonlinearity occurs, causing an oscillation, and as that oscillation propagates through the process it becomes less nonlinear. In this case however, the oscillation caused nonlinear trends to arise downstream of the root cause of the fault. Taking the trend of Level FT005 as an example, Figure 2a shows double peaks at each cycle.

Table 2. Start times of oscillations, indicating sequence of oscillation propagation.

Variable	**Start time [hh:mm:ss]**
Bank 1	
Level FT001	03:10:00
Level FT002	03:11:00
Level FT003	03:11:50
Level FT004	03:12:10
Level FT005	03:12:20
Level FT006	03:13:10
Level FT007	03:13:00
Bank 2	
Level FT008	03:10:10
Level FT009	03:10:40
Level FT010	03:11:50
Level FT011	03:11:40
Level FT012	03:12:20
Level FT013	03:12:20
Level FT014	03:10:50

Data-based diagnosis techniques have an inherent limitation in that they can only point to variables associated

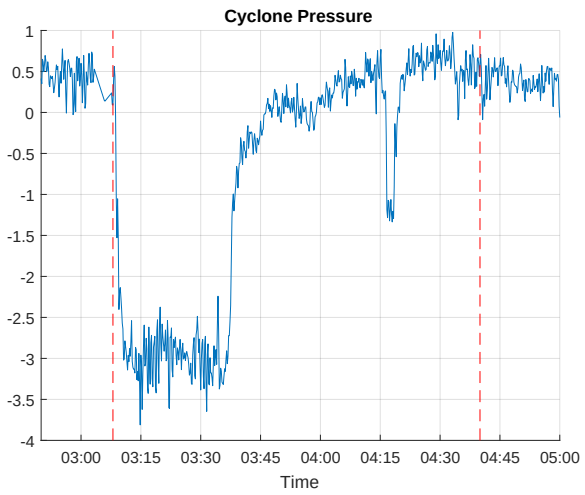

Fig. 4. Cyclone pressure just upstream of flotation circuit showing sharp dip at oscillation start at time 03:08:00.

with the root cause of the fault. Further analysis is needed to determine what caused the oscillation to manifest in that variable. Considering the unit just upstream of this flotation circuit, it was observed that the cyclone pressure decreased sharply just before the onset of the oscillation, as shown in Figure 4. This sudden drop may have caused the levels of the first cells in each bank (Level FT001 and Level FT008) to deviate from their set-points.

Further inspection also revealed that both the supervisory and optimisation advanced process control (APC) and the multivariable level controller were switched off for the duration of the oscillation. Only the base layer PID control, regulating the cell levels using the outflows from the cells, was enabled. This indicates that the regulatory control was unable to correct for the deviations in Level FT001 and Level FT008. Poor controller tuning may have caused the levels to become unstable and the absence of the multivariable controller allowed the resulting oscillations to propagate throughout the circuit. After the oscillations persisted for some time, the supervisory control level is switched back on to compensate for the oscillations by gradually changing the set points of the levels. This compensation is ineffective at first, but when the multivariable level controller is turned on again, the circuit quickly stabilises. This indicates that the multivariable controller is very effective at rejecting oscillations.

To summarise the findings of this analysis: transfer entropy indicated that the oscillation originated in Cells 1 and 8. This was confirmed by observing the sequence in which the oscillations appeared in each cell. A cyclone immediately upstream of the cells where the oscillation originated showed a sharp decrease in pressure, causing deviation of Level FT001 and Level FT008 from their set points. Suboptimal controller tuning may have resulted in the inability of the control to correct for these deviations, allowing the oscillation to propagate through the circuit.

5. CONCLUSIONS

An oscillation propagating through a flotation circuit was diagnosed using transfer entropy and the nonlinearity index. The two methods gave contradictory results. Considering knowledge of the material and control flow in the process, and the sequence of the oscillations in the system, it was concluded that the propagation path obtained using transfer entropy was accurate. The oscillation originated in, or just upstream of the first cells (Cells 1 and 8), in the flotation circuit. The nonlinearity index indicated that Level FT005 was closest to the sources of the oscillation. The nonlinearity index assumes that as an oscillation propagates through a process, appearing in different variables' time series, the trends become less nonlinear. In this case however, the oscillation caused nonlinear trends to arise downstream of the root cause of the fault.

The discrepancy in the results obtained for the two methods demonstrates the need to fully consider the assumptions of data-based techniques when interpreting their results. A universally applicable method for oscillation diagnosis is unlikely, with different techniques working for different scenarios. Understanding the limitations of techniques can lead to more successful and reliable applications of oscillation diagnosis strategies in industrial processes.

Once the correct propagation path had been identified further analysis was needed to determine what caused the oscillations in Cells 1 and 8. A cyclone immediately upstream of the cells where the oscillation originated showed a sharp decrease in pressure. This may have initiated the deviation of Level FT001 and Level FT008 from their set points. Suboptimal base layer controller tuning may have resulted in the inability of the control to correct for the fluctuations, allowing the oscillation to propagate through the circuit.

These results indicate that careful consideration of process knowledge is paramount to meaningful interpretation of the results from otherwise automated techniques.

The strengths and pitfalls of two popular oscillation diagnosis techniques were highlighted in this paper. Further research can focus on other popular techniques, such as Granger causality. Additionally, the combination of transfer entropy with an automated oscillation diagnosis strategy can be investigated to see how the techniques can be integrated.

REFERENCES

Bauer, M., Cox, J.W., Caveness, M.H., Downs, J.J., and Thornhill, N.F. (2007). Finding the Direction of Disturbance Propagation in a Chemical Process Using Transfer Entropy. *IEEE Transactions on Control Systems Technology*, 15(1), 12–21.

Bauer, M. and Thornhill, N.F. (2008). A practical method for identifying the propagation path of plant-wide disturbances. *Journal of Process Control*, 18(78), 707–719.

Duan, P. (2014). *Information Theory-based Approaches for Causality Analysis with Industrial Applications*. Thesis, University of Alberta.

Kantz, H. and Schreiber, T. (1997). *Nonlinear Time Series Analysis*. Cambridge University Press, New York, USA.

Landman, R. and J\"ams\"a-Jounela, S.L. (2016). Hybrid approach to casual analysis on a complex industrial system based on transfer entropy in conjunction with process connectivity information. *Control Engineering Practice*, 53, 14–23.

Muller, D., de Villiers, P.G.R., and Humphries, G. (2010). A Holistic Approach to Flotation Mass Pull and Grade Control. *IFAC Proceedings Volumes*, 43(9), 133–136.

Shumway, R.H. and Stoffer, D.S. (2014). *Time Series Analysis and Its Applications*. Springer.

Thornhill, N. (2005). Finding the source of nonlinearity in a process with plant-wide oscillation. *IEEE Transactions on Control Systems Technology*, 13(3), 434–443.

Thornhill, N.F. and Horch, A. (2007). Advances and new directions in plant-wide disturbance detection and diagnosis. *Special Issue - International Symposium on Advanced Control of Chemical Processes (ADCHEM) ADCHEM 2006 International Symposium on Advanced Control of Chemical Processes (ADCHEM)*, 15(10), 1196–1206.

Wills, B.A. and Finch, J.A. (2016). Chapter 12 - Froth Flotation. In *Wills' Mineral Processing Technology (Eighth Edition)*, 265–380. Butterworth-Heinemann, Boston.

Yang, F. and Xiao, D. (2012). Progress in Root Cause and Fault Propagation Analysis of Large-Scale Industrial Processes. *Journal of Control Science and Engineering*.

Yuan, T. and Qin, S.J. (2014). Root cause diagnosis of plant-wide oscillations using Granger causality. *Journal of Process Control*, 24(2), 450–459.